Hoshino, H. Uda, *Tetrahedron Lett.* **1997**, *38*, 6861 – 6864; c) J. Martin, M.-C. Lasne, J.-C. Plaquevent, L. Duhamel, *Tetrahedron Lett.* **1997**, *38*, 7181 – 7182; d) H. Kosugi, M. Abe, R. Hatsuda, H. Uda, M. Kato, *Chem. Commun*. **1997**, 1857 – 1858; e) T. Takahashi, N. Nakao, T. Koizumi, *Tetrahedron: Asymmetry* **1997**, *8*, 3293 – 3308; f) G. Asensio, P. A. Aleman, L. R. Domingo, M. Medio-Simón, *Tetrahedron Lett.* **1998**, *39*, 3277 – 3280; g) G. Asensio, P. Alemán, A. Cuenca, J. Gil, M. Medio-Simón, *Tetrahedron: Asymmetry* **1998**, *9*, 4073 – 4078; h) H. Fujihara, K. Tomioka, *J. Chem. Soc. Perkin Trans. 1* **1999**, 2377 – 2381; i) Y. Nakamura, S. Takeuchi, Y. Ohgo, D. P. Curran, *Tetrahedron* **2000**, *56*, 351 – 356.

[3] Enantioselective protonation by catalytic antibodies: a) I. Fujii, R. A. Lerner, K. D. Janda, *J. Am. Chem. Soc.* **1991**, *113*, 8528 – 8259; b) J.-L. Reymond, J.-L. Reber, R. A. Lerner, *Angew. Chem.* **1994**, *106*, 485 – 486; *Angew. Chem. Int. Ed. Engl*. **1994**, *33*, 475 – 477.

[4] a) A. Yanagisawa, T. Kikuchi, T. Watanabe, T. Kuribayashi, H. Yamamoto, *Synlett* **1995**, 372 – 374; b) A. Yanagisawa, T. Watanabe, T. Kikuchi, H. Yamamoto, *J. Org. Chem.* **2000**, *65*, 2979 – 2983.

[5] K. Ishihara, S. Nakamura, M. Kaneeda, H. Yamamoto, *J. Am. Chem. Soc*. **1996**, *118*, 12854 – 12855.

[6] Y. Nakamura, S. Takeuchi, A. Ohira, Y. Ohgo, *Tetrahedron Lett*. **1996**, *37*, 2805 – 2808.

[7] J. Muzart, F. Hénin, S. J. Aboulhoda, *Tetrahedron: Asymmetry* **1997**, *8*, 381 – 389.

[8] a) P. Riviere, K. Koga, *Tetrahedron Lett*. **1997**, *38*, 7589 – 7592; b) E. Vedejs, A. W. Kruger, *J. Org. Chem*. **1998**, *63*, 2792 – 2793; c) E. Vedejs, A. W. Kruger, N. Lee, S. T. Sakata, M. Stec, E. Suna, *J. Am. Chem. Soc.* **2000**, *122*, 4602 – 4607; d) Y. Yamashita, Y. Emura, K. Odashima, K. Koga, *Tetrahedron Lett.* **2000**, *41*, 209 – 213.

[9] For the use of transient enolates or enols in catalytic asymmetric protonation, see: a) H. Pracejus, F.-W. Wilcke, K. Hanemann, *J. Prakt. Chem.* **1977**, *319*, 219 – 229; b) N. Kobayashi, K. Iwai, *Polym. J.* **1981**, *13*, 263 – 271; c) A. Kumar, R. V. Salunkhe, R. A. Rane, S. Y. Dike, *J. Chem. Soc. Chem. Commun*. **1991**, 485 – 486; d) F. Toda, K. Tanaka, J. Sato, *Tetrahedron: Asymmetry* **1993**, *4*, 1771 – 1774; e) C. Fehr, I. Stempf, J. Galindo, *Angew. Chem.* **1993**, *105*, 1093 – 1095; *Angew. Chem. Int. Ed. Engl.* **1993**, *32*, 1044 – 1046.

[10] For the use of chiral binaphthol derivatives as a chiral proton source, see: a) E. Emori, T. Arai, H. Sasai, M. Shibasaki, *J. Am. Chem. Soc.* **1998**, *120*, 4043 – 4044; b) E. Emori, T. Iida, M. Shibasaki, *J. Org. Chem.* **1999**, *64*, 5318 – 5320.

[11] K. Nishimura, M. Ono, Y. Nagaoka, K. Tomioka, *J. Am. Chem. Soc.* **1997**, *119*, 12974 – 12975.

[12] a) U. Schmidt, E. Öhler, *Angew. Chem.* **1976**, *88*, 54; *Angew. Chem. Int. Ed. Engl.* **1976**, *15*, 42; b) J. Keniya, A. A. Natu, V. N. Gogte, *Chem. Ind.* **1986**, 243; c) J. R. Mohrig, S. S. Fu, R. W. King, R. Warnet, G. Gustafson, *J. Am. Chem. Soc.* **1990**, *112*, 3665 – 3667; d) O. Miyata, T. Shinada, I. Ninomiya, T. Naito, T. Date, K. Okamura, S. Inagaki, *J. Org. Chem*. **1991**, *56*, 6556 – 6564; e) Y. Kita, N. Shibata, T. Miki, Y. Takemura, O. Tamura, *Chem. Pharm. Bull.* **1992**, *40*, 12 – 20; f) J. R. Mohrig, R. E. Rosenberg, J. W. Apostol, M. Bastienaansen, J. W. Evans, S. J. Franklin, C. D. Frisbie, S. S. Fu, M. L. Hamm, C. B. Hirose, D. A. Hunstad, T. L. James, R. W. King, C. J. Larson, H. A. Latham, D. A. Owen, K. A. Stein, R. Warnet, *J. Am. Chem. Soc.* **1997**, *119*, 479 – 486.

[13] a) B. Dmuchovsky, B. D. Vineyard, F. B. Zienty, *J. Am. Chem. Soc.* **1964**, *86*, 2874 – 2877; b) H. Hiemstra, H. Wynberg, *J. Am. Chem. Soc*. **1981**, *103*, 417 – 430.

[14] K. Tomioka, M. Okuda, K. Nishimura, S. Manabe, M. Kanai, Y. Nagaoka, K. Koga, *Tetrahedron Lett.* **1998**, *39*, 2141 – 2144.

[15] Direct HPLC analysis of **4c** (Ar = 2-TMSPh, R = Ph) sometimes did not afford a clear base line separation. The protodesilylated product (Ar = R = Ph) gave a base line separation that was adequate for determining the *ee* value.

[16] a) W. A. Bonner, J. A. Zderic, *J. Am. Chem. Soc.* **1956**, *78*, 3218 – 3221; b) H. Pracejus, *Liebigs Ann. Chem*. **1960**, *634*, 9 – 22.

[17] R. Baker, M. J. O'Mahony, C. J. Swain, *J. Chem. Soc. Perkin Trans. 1* **1987**, 1623 – 1633.

[18] M. Kobayashi, K. Koga, S. Yamada, *Chem. Pharm. Bull*. **1972**, *20*, 1898 – 1905.

[19] R. Menicagli, O. Piccolo, L. Lardicci, M. L. Wis, *Tetrahedron* **1979**, *35*, 1301 – 1306.

[20] a) O. Piccolo, F. Spreafico, G. Visentin, *J. Org. Chem*. **1987**, *52*, 10 – 14; b) I. T. Harrison, B. Lewis, P. Nelson, W. Rooks, A. Roszkowski, A. Tomolonis, J. H. Fried, *J. Med. Chem*. **1970**, *13*, 203 – 205.

[21] Since the lithium atom of the transient enolate **3** is complexed with the chiral amino diether ligand **2**, one can speculate that the enantioselective protonation takes place under the control of the ligand. However, the attempted protonation of a lithium enolate, generated from TMS enol ether and methyllithium in the presence of a stoichiometric amount of **2**, with 2-TMS-benzenethiol gave rather poor selectivity.

Synthesis of Nanophase Iron Oxide in Lumazine Synthase Capsids**

Wayne Shenton, Stephen Mann,* Helmut Cölfen, Adelbert Bacher,* and Markus Fischer

The ability to control the crystallization of inorganic materials at the nanometer length scale has prompted the use of self-assembled "nanoreactors" such as surfactant[1] and block copolymer[2] micelles, liquid crystalline mesophases,[3] and porous two-dimensional protein crystals.[4] In general, these systems consist of spatially confined environments that are topologically distinct and comprise nucleation sites which direct the growth of the inorganic phase. A biological archetype of this strategy is the protein ferritin, in which iron oxide nanoparticles are synthesized within an 8-nm-diameter hollow polypeptide cage.[5] It has previously been shown that this bio-nanoreactor can be used to produce a number of dispersed protein – inorganic nanocomposites[6–8] that have potential applications in medical imaging[9] and neutron capture therapy.[10] The utilization of other biomolecular systems analogous to ferritin could have important implications for the development of a general class of self-assembled bioinorganic materials with designed functionality and biocompatibility. For example, viral capsids have been recently used to synthesize inorganic-based nanoparticles.[11] Herein we describe a new type of bio-nanoreactor based on the enzyme lumazine synthase which can be utilized for the biomimetic synthesis of iron oxide nanoparticles, even though there is no evidence for such a function in vivo.

[*] Prof. S. Mann, Dr. W. Shenton
School of Chemistry
University of Bristol
Bristol BS8 1TS (UK)
Fax: (+44) 117-929-0509
E-mail: s.mann@bris.ac.uk
Dr. H. Cölfen
Max-Planck Institute of Colloids and Interfaces
Am Mühlenberg 2, 14476 Golm (Germany)
Prof. A. Bacher, Dr. M. Fischer
Lehrstuhl für Organische Chemie und Biochemie
Technischen Universität München
Lichtensbergstrasse 4, 8046 Garching (Germany)
E-mail: adelbert.bacher@ch.tum.de

[**] This work was supported by the BBSRC (W.S.). We thank A. M. Seddon for help with transmission electron microscopy and analytical ultracentrifufation studies and G. D. Ruggiero for the generation of computer images.

  1433-7851/01/4002-0442 $ 17.50+.50/0

Lumazine synthase is a hollow 1 MDa bacterial enzyme complex of 60 subunits that is involved in the synthesis of lumazine, a precursor to riboflavin. The structure of lumazine synthase from *Bacillus subtilis* has recently been elucidated and the X-ray structure analysis confirms it has a hollow porous shell with icosahedral ($T=1$) morphology and inner and outer diameters of 7.8 nm and 14.7 nm, respectively (Figure 1).[12] The intersubunit contacts of the capsid consist of dimers, trimers, and pentamers. The trimer contacts are formed by several segments at the inner capsid wall (residues 21–29, 81–85, 120–143) that produce a contact region consisting of a cluster of three glutamic acid residues.[13] As there are no compensating ligands, a large negative charge density exists on the inner wall of the capsid. Interestingly, similar domains of negative charge are present in ferritin and may act as nucleation sites for iron oxide deposition.[5] The interior of the lumazine synthase capsid is accessed through hydrophilic funnel-shaped channels lined with glutamic acid residues, and located at the ten threefold axes. Channels are also formed along the six fivefold pentamer axes,[12] and consist of symmetrically arranged α-helices, reminiscent of membrane channel proteins. The inner surface of these pores is dominated by polar residues, which have been implicated in substrate import and product export from the catalytic centers of the enzyme.[14] The compact nature of the capsid structure implies the channels have a significant role in substrate exchange.[15]

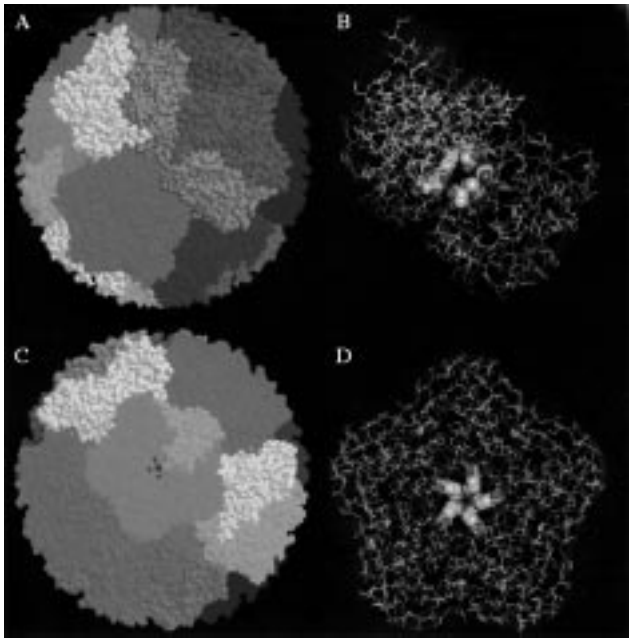

Figure 1. Computer-generated images of lumazine synthase. A) View down the threefold channel of the enzyme. B) View highlighting the glutamic acids lining the threefold channel. C) View down the fivefold channel. d) View highlighting the lysine residues lining the fivefold channel.

Previous work[13] has shown that the lumazine synthase capsid possesses 60 substrate binding sites at the pentamer interfaces. These binding sites are located on the inner wall and consequently the stability of the capsid is dependent upon the presence of the substrate (5-nitro-6-ribitylamino-2,4(1*H*,3*H*)-pyrimidinedione) or substrate analogues. The 15-nm-diameter capsid is highly stable at pH 7 in the presence of phosphate buffer and substrate analogues (Figure 2 A). In the absence of these ligands, however, the structure can dynamically rearrange into larger forms, notably a $T=3$ icosahedron containing 240 subunits, but depends on the buffer composition and pH.[16]

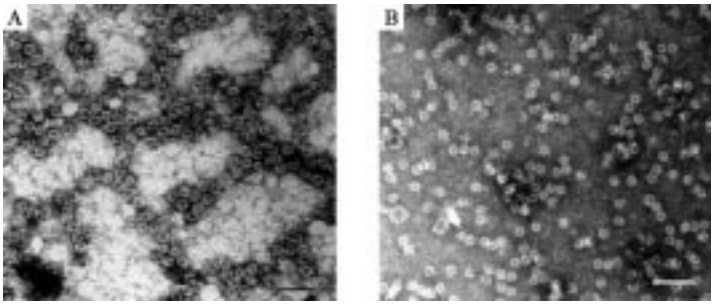

Figure 2. TEM images of negatively stained lumazine synthase showing hollow spherical 15-nm-diameter capsids infiltrated with uranyl acetate: A) in phosphate buffer, scale bar 50 nm, and B) 24 h after addition to MES buffer at pH 6.5 showing the presence of a few larger capsids with diameters of 30 nm (arrow). Scale bar 50 nm.

To investigate the potential of lumazine synthase as a nanoreactor for iron oxide mineralization we prepared protein solutions in 4-morpholine-ethanesulfonic acid (MES) buffer at pH = 6.5 in the absence of substrate molecules. Transmission electron microscopy (TEM) images of samples stained with uranyl acetate indicated that the 15-nm-diameter capsids were stable under these conditions, although some larger structures (about 5% of the population) with external and internal diameters of about 30 and 20 nm, respectively were occasionally observed (Figure 2 B). The synthesis of iron oxide in these solutions was undertaken by adding aliquots of a 1 mM de-aerated solution of aqueous Fe^{II} ions stepwise in air to a de-aerated enzyme solution (0.1 mg mL^{-1}, MES buffer, pH 6.5). Typically, aliquots of approximately 1.7 Fe^{II} ions per subunit (100 Fe^{II} ions per capsid) were added every 15 minutes to give final theoretical loadings of 5, 17, 25, and 33 Fe ions per subunit (300, 1000, 1500, and 2000 Fe atoms per 15-nm diameter capsid). Control experiments with identical concentrations of Fe^{II} ions but without the enzyme were also undertaken. Significantly, whereas the control solutions turned red-brown and produced a bulk precipitate as a result of slow aerial oxidative hydrolysis and condensation of Fe^{II} ions to Fe^{III} oxide, the protein solutions remained transparent and free from sediment. The corresponding UV/Vis spectra (Figure 3) recorded 24–48 h after the addition of the final aliquot of Fe^{II} ions showed a single broad absorption band extending to 550 nm for the control solutions, but a distinct absorption edge at 400 nm as well as an absorption at 270 nm corresponding to an aromatic amino acid side chain for the lumazine synthase solutions. The red-brown colour of the control samples is characteristic of extended arrays of polynuclear oxo- and hydroxo-bridged Fe^{III} centers such as is observed for the fully formed ferrihydrite cores of ferritin. In contrast, the strong

  1433-7851/01/4002-0443 $ 17.50+.50/0

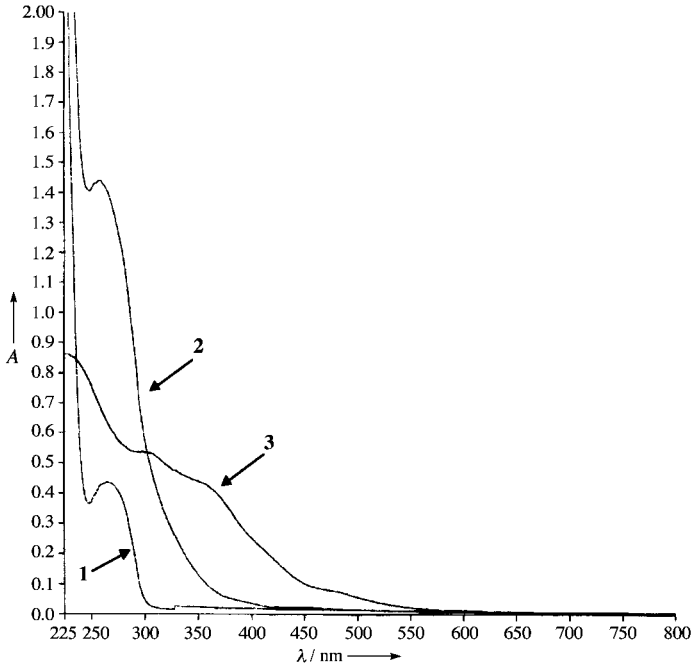

Figure 3. UV/Vis spectra of lumazine synthase: 1) in MES buffer prior to the addition of Fe^{II} ions showing an absorbance at 270 nm from the aromatic side chains; 2) 24 h after the addition of a total of 5 Fe atoms per subunit (300 Fe atoms per capsid); and 3) control sample, which corresponds to the experimental conditions of (2), but without protein.

absorption in the UV region observed for the iron-containing lumazine synthase solutions is indicative of relatively low molecular weight Fe^{III}-containing clusters with incomplete bridging ligands which are possibly associated with protein side chains.[17]

TEM images and corresponding energy dispersive X-ray (EDX) analysis of unstained samples of Fe-loaded lumazine synthase solutions showed the presence of iron-containing electron-dense nanoparticles. At a loading of five Fe atoms per subunit the particles were diffuse, low in contrast, and heterogeneous in shape and size (Figure 4 A). Most particles were less than 30 nm in dimension. Selected area electron diffraction (SAED) patterns showed weak and broad concentric rings with d spacings of 0.32, 0.19, and 0.17 nm corresponding to the (021), (002), and (151) reflections of the iron(III) oxide mineral lepidocrocite (γ-FeOOH). Similar results were obtained at a higher loading of 17 Fe atoms per subunit except that the γ-FeOOH nanoparticles were more electron dense and crystalline (d spacings, 0.32, 0.19, 0.17, and 0.152 nm; Figure 4 C). The particles were between 10 and 15 nm in size (mean = 13.4 nm, σ = 2.0 nm). In contrast, no nanoparticles were observed in samples prepared in the absence of lumazine synthase. Instead, the TEM analysis showed micrometre-sized plate-shaped particles of lepidocrocite (data not shown).

The presence of lumazine synthase capsids in the Fe-loaded samples was confirmed by staining the air-dried samples with uranyl acetate (Figures 4 B, D). Particle size measurements on samples prepared with a loading of 17 Fe atoms per subunit showed a broad distribution of capsid diameters centred around values of 15 and 30 nm, which corresponds to about 30 and 70 % of the population, respectively. The results suggest

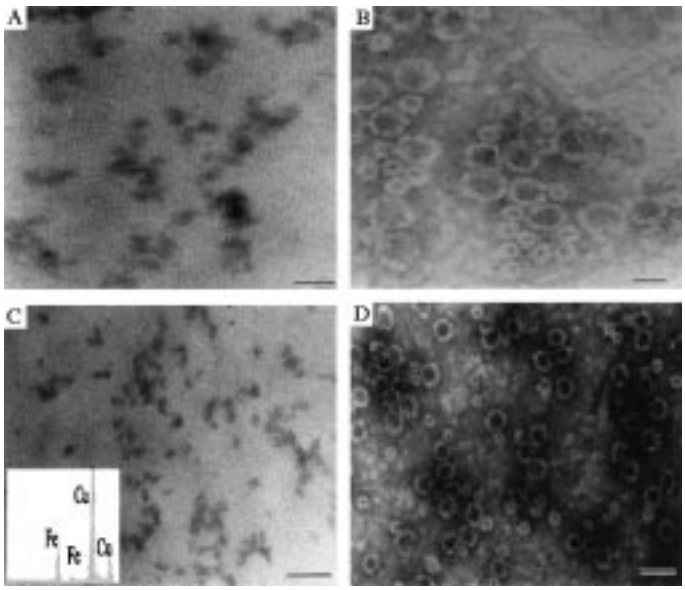

Figure 4. TEM images of iron oxide mineralized lumazine synthase samples, approximately 48 h after the addition of the final aliquot of Fe^{II} ions to the protein solutions. A) and C) Unstained samples prepared with a loading of 5 and 17 Fe atoms, respectively, per subunit showing the presence of iron oxide nanoparticles; scale bars = 30 nm and 50 nm, respectively. The inset in C) shows the corresponding EDX, which confirms the presence of Fe ions (the Cu comes from the TEM grid). B) and D) Negatively stained images of the samples shown in A) and C), respectively, showing the presence of a mixed population of capsids with diameters centred around 30 and 15 nm; scale bars = 30 and 50 nm, respectively.

that the 15-nm-diameter native form of the lumazine synthase capsids is to some extent destabilized in the presence of Fe^{III} ions and replaced by intact capsids with larger diameters. The latter have diameters around 30 nm, which is comparable to those previously measured for a $T = 3$ icosahedral form of lumazine synthase.[16]

Analytical ultracentrifugation (AUC) analysis of a solution of lumazine synthase in MES buffer showed a single species with a well-defined sedimentation coefficient ($s_{20,w}$) of 23.0 S (Figure 5), which was slightly lower than the published value

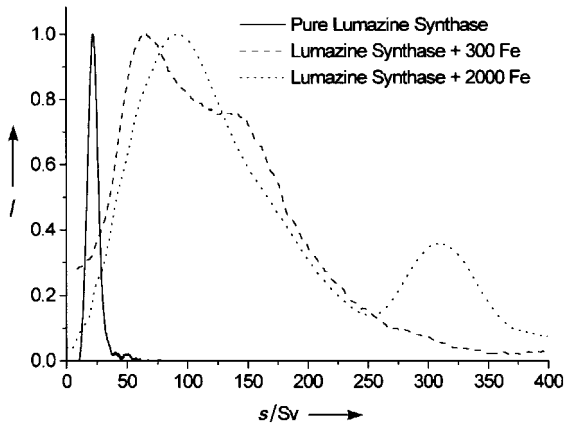

Figure 5. Apparent sedimentation coefficient distributions for lumazine synthase solutions prepared with a loading of 5 Fe or 33 Fe atoms per subunit (300 or 2000 Fe atoms per capsid, respectively) at 25 °C in MES buffer. The samples were analyzed several days after the addition of the final aliquot of Fe^{II} ions to the protein solution. I = Intensity.

  1433-7851/01/4002-0444 $ 17.50+.50/0 *Angew. Chem. Int. Ed.* **2001**, *40*, No. 2

of 26 S,[17] probably because of the concentration dependence of sedimentation. Only a very small peak was observed at $s_{20,w} = 48$ S, which confirmed that the 15-nm capsid was stable in MES buffer. In contrast, the Fe-loaded lumazine synthase solutions showed the presence of a broadened spread of sedimentation coefficients at significantly higher S values, which suggests that there were significant heterogeneities in the extent of iron loading or structure of the higher aggregates, or both (Figure 5). At a loading of five Fe atoms per subunit the sedimentation coefficient distribution showed no distinct peak corresponding to the native 15-nm capsid; instead, a broad distribution with a major peak at $s_{20,w} = 67$ S and a shoulder at 138 S were observed (Figure 5). The former is close to the 70 S species previously observed for lumazine synthase under conditions of capsid reorganization,[18] which suggests that this component corresponds to higher order capsids that are iron-free or associated with only low levels of iron oxide. The shoulder at 138 S, on the other hand, probably represents a wide distribution of the same structures with significant iron oxide cores. Similar broad density distributions were observed for higher iron loadings with a concomitant shift in the S value for the peak maxima (Figure 5).

The results indicate that the bulk precipitation of Fe^{III} oxide is strongly inhibited in the presence of lumazine synthase because the mineral phase is specifically encapsulated within the internal cavity of the capsid. Interactions between the enzyme and iron appear to destabilize the native capsid, which then transforms into a higher order structure in association with discrete nanoparticles of iron oxide. The nature of this rearrangement remains unclear, but previous results[18] have suggested that the formation of 30-nm diameter capsids involves the assembly of 240 subunits. In general, iron atoms could permeate the porous shell of the capsids by diffusion through the threefold channel lined with glutamic acid residues. Ion binding at the anionic domains on the inner wall would then increase the rate of nucleation specifically within the internal cavity by lowering the interfacial energy of the critical nucleus formed from oxidative hydrolysis. Growth of the nucleus is likely to be autocatalytic because the iron oxide phase promotes further oxidation of Fe^{II} ions directly on the surface of the developing nanoparticle. This explains the "all or nothing" distribution of nanoparticles in which a subset of molecules contain a high iron loading whilst other capsids remain effectively empty.

In conclusion, this work has shown for the first time that lumazine synthase, a hollow enzyme found in bacteria and fungi, can serve as a mineralization template in the fabrication of nanocrystalline iron oxide. The presence of positive and negatively charged channels in the capsid shell suggests that it might be possible to simultaneously sequester both cationic and anionic reactants for the synthesis of other types of inorganic nanoparticles besides iron oxides for potential uses in electronic, optical, or magnetic devices.

Experimental Section

Droplets (5 μL) of lumazine synthase solutions (10 and 0.1 mg mL^{-1}) in phosphate (pH 7) or MES (Aldrich) buffer adjusted to pH 6.5 by addition of 0.1M NaOH were blotted dry onto formvar-covered carbon-coated copper TEM grids and imaged in a JEOL 2000FX analytical TEM. Some grids were stained with a 2% aqueous uranyl acetate solution for 1 min and washed several times with distilled water. Similar methods were used with concentrated iron-containing lumazine synthase solutions prepared in a centrifugal filtration device (10 kDa cut off, Millipore Ltd).

The iron oxide mineralization protocol was as follows: A 1 mM solution of $(NH_4)_2SO_4 \cdot FeSO_4 \cdot 6H_2O$ was prepared and de-aerated under N_2 for 30 min prior to the start of the mineralization experiment. The aqueous stock solution of Fe^{II} ions was kept under N_2 for the duration of the experiment. A 0.1 mg mL^{-1} solution of lumazine synthase in MES was de-aerated for 15 mins under N_2, after which the gas was removed and aliquots of the Fe^{II} solution added with slow stirring. Phosphate buffers were not used since they strongly complex aqueous Fe^{II} ions. Typically, aliquots of 100 Fe^{II} ions per native capsid were added in air every 15 min with a microsyringe to give final theoretical loadings of 5, 17, 25, and 33 Fe atoms per subunit (300, 1000, 1500, and 2000 Fe atoms per capsid). The addition of each volume of Fe^{II} ions was undertaken slowly over a period of 10 s to ensure slow aerial oxidation. After the final addition, the protein solutions were stirred at room temperature for 24 h. Typically, samples were analysed by TEM approximately 48 h after the addition of the final aliquot of Fe^{II} ions to the protein solutions. Control experiments with identical concentrations of Fe^{II} ions but without the enzyme were undertaken.

UV/Vis spectra were recorded using a Perkin Elmer UV/Vis spectrophotometer and spectra displayed using the Lambda 11 software package. Samples were analyzed at regular intervals (every 2 h) by transfer of 3-mL aliquots from the reaction vessel to quartz cuvettes. Samples were returned to their respective reaction vessels before further aliquots of Fe^{II} ions were added. Spectra were also recorded 24–48 h after the addition of the final aliquot of Fe^{II} ions to the protein solution.

Samples were analyzed by analytical ultracentrifugation several days after the addition of the final aliquot of Fe^{II} ions to the protein solution using a Beckman Optima XL-I (Beckman-Coulter, Palo Alto, CA) with UV/Vis absorption optics at 280 nm. The solutions were investigated in 12-mm self-made double-sector titanium centrepieces at 25 °C and 20000 RPM (pure protein, and protein + 5 Fe atoms per subunit) and 10000 RPM (protein + 33 Fe atoms per subunit). Apparent sedimentation coefficient distributions were recorded using the time derivative method.[19] The sedimentation coefficients were not corrected to infinite dilution.

Received: September 7, 2000
Revised: October 10, 2000 [Z15775]

[1] A. P. Alivisatos, *Science* **1996**, *271*, 933–937.
[2] L. Bronstein, E. Kraemer, B. Berton, C. Burger, S. Foerster, M. Antonietti, *Chem. Mater.* **1999**, *11*, 1402–1405.
[3] P. V. Braun, S. I. Stupp, *Mater. Res. Bull.* **1999**, *34*, 463–469.
[4] W. Shenton, D. Pum, U. B. Sleytr, S. Mann, *Nature* **1997**, *389*, 585–587.
[5] P. M. Harrison, P. J. Artymuik, G. C. Ford, D. M. Lawson, J. M. A. Smith, A. Treffry, J. L. White in *Biomineralization: Chemical and Biochemical Perspectives* (Eds.: S. Mann, J. Webb, R. J. P. Williams), VCH, Weinheim, **1989**, pp. 257–294.
[6] F. C. Meldrum, B. R. Heywood, S. Mann, *Science* **1992**, *257*, 522–523.
[7] T. Douglas, D. P. E. Dickson, S. Betteridge, J. Charnock, C. D. Garner, S. Mann, *Science* **1995**, *269*, 54–57.
[8] K. K. W. Wong, S. Mann, *Adv. Mater.* **1996**, *8*, 928–934.
[9] M. Zborowski, B. F. Chwan, G. Green, N. Baldwin, S. Reddy, T. Douglas, S. Mann, J. Chalmers, *Cytometry* **1996**, *24*, 251–259.
[10] J. F. Hainfield, *Proc. Natl. Acad. Sci. USA* **1992**, *89*, 11064–11068.
[11] T. Douglas, M. Young, *Nature* **1998**, *393*, 152–155.
[12] R. Ladenstein, M. Schneider, R. Huber, H. D. Bartunik, K. Wilson, K. Schott, A. Bacher, *J. Mol. Biol.* **1988**, *203*, 1045–1070.
[13] K. Ritsert, R. Huber, D. Turk, R. Ladenstein, K. Schmidt-Bäse, A. Bacher, *J. Mol. Biol.* **1995**, *253*, 151–167.
[14] R. Ladenstein, A. Bacher, R. Huber, *J. Mol. Biol.* **1987**, *195*, 751–753.
[15] K. Kis, A. Bacher, *J. Biol. Chem.* **1995**, *270*, 16788–16795.
[16] K. Schott, R. Ladenstein, A. König, A. Bacher, *J. Biol. Chem.* **1990**, *265*, 12686–12689.
[17] I. Macara, T. G. Hoy, P. M. Harrison, *Biochem. J.* **1973**, *82*, 396.
[18] A. Bacher, H. Ludwig, H. Schnepple, Y. Ben-Shaul, *J. Mol. Biol.* **1986**, *187*, 75–86.
[19] W. F. Stafford, *Anal. Biochem.* **1992**, *203*, 295–301.

  1433-7851/01/4002-0445 $ 17.50+.50/0